FOSSEE, IIT Bombay
OpenFOAM Case Study Project
Summer Fellowship
July, 2025

Optimizing hole distribution in a showerhead of a semiconductor reactor

Supraja Shinde[1]

Department of Aerospace Engineering MIT ADT University Loni Kalbhor, Pune, Maharashtra

Guides:

Dr Ajit Balakrishna

Sr. Director, CAE PMTS at Applied Materials, USA.

Prof. Himani Garg

Assistant Professor, Lund University, Sweden.

Prof. Raghvendra Gupta

Professor at Indian Institute of Technology, Guwahati

Mentor: Mr. Manjil Sitoula

FOSSEE IIT Bombay

Abstract

This study presents a computational investigation aimed at optimizing the showerhead design in a Halogen Chemical Vapor Deposition (HCVD) reactor using OpenFOAM. The work focuses on enhancing gas flow uniformity across the substrate, which is essential for achieving high-quality and uniform thin-film deposition. Various geometric configurations were examined, including logarithmic hole distribution patterns in the showerhead and different baffle sizes (8 mm and 16 mm). Simulation results demonstrated that while the inclusion of a showerhead improves gas redistribution, it does not fully mitigate the dominance of central jet impingement. However, increasing the baffle size from 8 mm to 16 mm significantly reduced jet intensity at the centre and promoted more effective lateral flow spreading across the substrate. These findings highlight the critical role of geometric optimization in improving flow uniformity.

Keywords: Chemical Vapour Deposition, Showerhead, Substrate, Baffle.

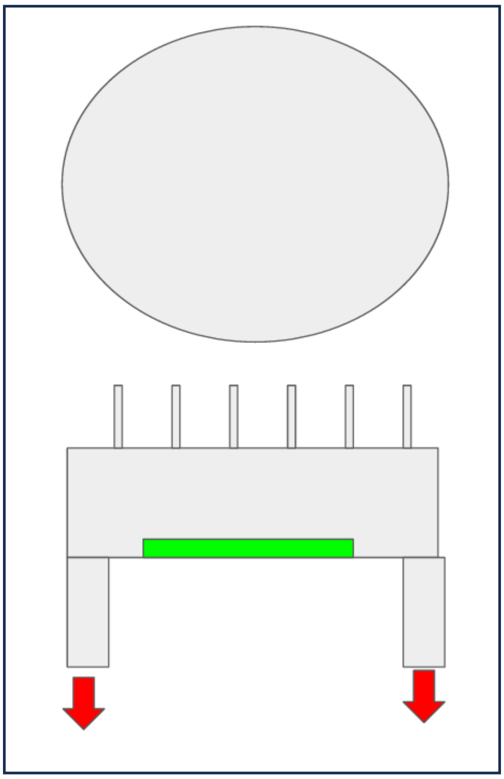

Fig 1: Schematic of the wafer and showerhead

1. Introduction

Chemical Vapor Deposition (CVD) is a vital process in semiconductor manufacturing used for depositing high-quality thin films on wafers. In a Halogen Chemical Vapor Deposition (HCVD) system, achieving uniform gas distribution is essential to ensure consistent and defect-free film growth. The showerhead, positioned above the wafer, plays a key role in distributing reactant gases evenly. Its geometric design-particularly the size, spacing, and distribution pattern of the holes-significantly impacts flow behaviour within the chamber. Any imbalance can lead to non-uniform deposition, ultimately affecting device performance. Therefore, optimizing the showerhead design is critical for enhancing process efficiency and ensuring uniform film deposition across the wafer.

In this case study, the primary focus is to optimize the flow through the showerhead and analyse flow behaviour using various simulation case studies. The aim is to evaluate how different geometric and operational parameters influence gas distribution and deposition uniformity. By examining configurations involving hole patterns, baffle distances, and substrate positioning, the study seeks to enhance gas dispersion and improve deposition outcomes using CFD tools in OpenFOAM.

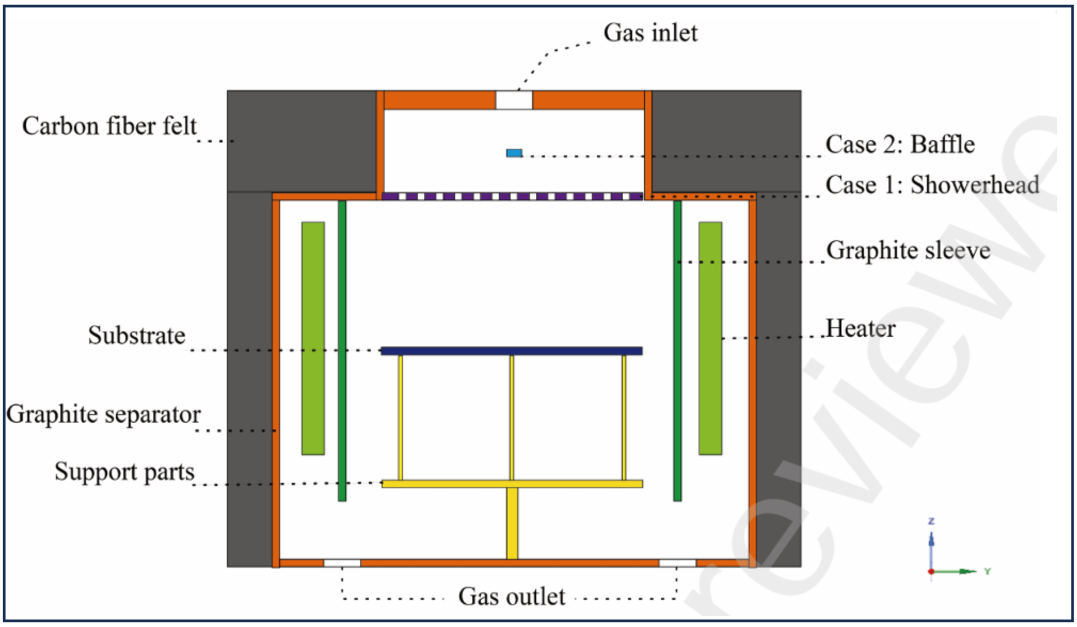

Fig. 1.1: Schematic of the Halogen Chemical Vapor Deposition (HCVD) Chamber [2]

2. Literature Review

A study explored the influence of various showerhead hole patterns on gas flow in a Plasma Enhanced CVD reactor. As the whole density of the centre region increased the pressure of the centre in the gas distribution space increased ,the velocity gradient of the centre in the process volume increased and local residence time of the centre decreased .This study highlights the importance of hole distribution in achieving uniform film deposition through precise flow control [1].The CFD was used to study the effect of showerhead structure and baffle on the deposition rate of substrate surface. As the size and position of holes are optimized, film uniformity improves [2]. A study developed a machine learning-driven optimization framework for showerhead design in semiconductor deposition, integrating CFD-informed surrogate models to achieve high flow uniformity. Using Bayesian optimization, the approach outperformed traditional methods while requiring significantly fewer simulations. This highlights the potential of combining machine learning and CFD to streamline design processes and improve efficiency. The framework demonstrates strong promise not only for optimizing showerhead configurations but also for broader applications across manufacturing systems, including additive manufacturing and thermal process control, where rapid and accurate design decisions are essential for achieving consistent performance and reducing development time [3]. A novel CVD reactor design featuring a segmented, reverse-flow showerhead was introduced to enable spatial control of gas composition across the wafer surface. A three-segment prototype successfully demonstrated patterned film deposition, which in turn guided further simulation development. This modular showerhead system offers enhanced control over deposition uniformity, supports combinatorial material studies, and allows for scalability to larger substrate sizes. The design enables independent control of gas zones, improving process flexibility. Ongoing research focuses on refining gas delivery precision and improving manufacturability, highlighting the potential of segmented showerheads for advanced semiconductor fabrication and customized thin-film deposition processes [4]. A CFD study conducted on a showerhead-type capacitively coupled plasma (CCP) reactor revealed that electrode spacing significantly affects particle deposition behavior. When the electrode spacing is smaller, particles are more likely to deposit directly from the showerhead onto the substrate. In contrast, larger electrode spacing promotes deposition primarily from plasma-generated particles. These findings emphasize the impact of reactor geometry on deposition mechanisms and process outcomes. The study provides valuable insight into how showerhead and electrode design influence particle transport. Future work aims to incorporate discharge modeling and investigate the effects of non-spherical particle motion for more accurate process simulations [5]. A 3D finite volume simulation was employed to optimize Hot Filament Chemical Vapor Deposition (HFCVD) parameters, focusing on the arrangement of filaments and gas inlets to achieve uniform temperature and gas density distribution. The study identified optimal design parameters-number of filaments (N=6), filament radius (r=0.4 mm), filament spacing (D=16-18 mm), and height above substrate (H=8-9 mm) that led to uniform substrate temperatures and enhanced film growth conditions. Experimental validation confirmed the successful deposition of homogeneous, fine-faceted diamond films on Si wafers, highlighting the effectiveness of numerical simulation in guiding reactor design for improved film quality and process efficiency [6]. A study modeled multiphase systems in plasma environments by treating each phase as a gas with phase exchange occurring under low pressure and temperature conditions. The approach decouples the complex multiphase problem into simpler single-phase sub-models, which are then iteratively coupled to simulate the complete system. This method effectively captures key physical phenomena such as sorption effects while maintaining computational efficiency. By reducing splitting errors and enhancing solver stability, the model enables more accurate simulations of plasma-assisted deposition processes. The technique highlights the potential of modular modeling in handling complex multiphase interactions in chemically reactive and low-pressure environments [7]. A study introduced the Profile Error Feedback (PEF) optimization method for designing vector showerheads in vertical CVD reactors, enabling precise control over gas velocity profiles across the substrate. By modeling the showerhead face plate as a porous medium, the method simplifies the complex flow behaviour while maintaining accuracy. The approach iteratively adjusts design parameters to minimize deviations from the target velocity distribution, allowing for near-uniform gas flow with significantly fewer design iterations. This optimization strategy demonstrates high efficiency and effectiveness in achieving flow uniformity, making it a promising tool for enhancing film deposition quality in advanced semiconductor manufacturing [8].

3. Governing Equations

The SimpleFoam solver in OpenFOAM is a steady-state, incompressible, and turbulent flow solver based on the SIMPLE (Semi-Implicit Method for Pressure Linked Equations) algorithm. It is widely used for internal and external aerodynamic simulations where compressibility effects are negligible.

The fluid dynamics are governed by the conservation equations of mass, momentum, and energy, supplemented by the ideal gas law to relate pressure, temperature, and density:

- Continuity Equation (Mass Conservation):

$$\frac{dp}{dt} + \nabla \cdot (\rho \boldsymbol{u}) = 0$$

where ρ is the fluid density and u is the velocity vector.

- Momentum Equation:

$$\nabla \cdot (\rho \boldsymbol{u}\boldsymbol{u}) = -\nabla p + \nabla \cdot (\mu_{eff} \nabla \boldsymbol{u}) + \rho g$$

where ρ is the fluid density,u is the velocity vector, μ_{eff} is the effective dynamic viscosity, ∇p is the pressure gradient force, p is the static pressure, g is the gravitational acceleration.

- Equation of State (Perfect Gas Law):

$$p = \rho RT$$

where p is the static pressure, ρ is the fluid density, R is the specific gas constant, Tis the temperature.

4. Simulation Procedure

4.1. Computational Domain

To accurately capture the flow characteristics, an appropriate computational domain is created representing the physical geometry of the problem under investigation. The design of the geometry plays a crucial role in ensuring that the boundary conditions and flow features are represented realistically.

4.1.1. Computational domain of the 3D Halogen Chemical Vapor Deposition (HCVD) Chamber.

- Components of the 3-D HCVD

(i)Inlet:

The inlet has an important function in a CVD reactor, especially for laminar flow regimes, where regular and smooth gas motion can be crucial for efficient deposition control. It feeds process gases such as carriers and precursors to the chamber and has a considerable starting flow structure impact. For laminar flows, it must be carefully designed to minimize disturbances and generate a stable, uniform, and parallel flow of gases to the reactor. Any form of asymmetry or extreme variation in flow direction at the inlet can disturb the laminar profile and create unsuitable gradients in velocity and concentration. An adequately developed inlet can generate a stable and evenly distributed flow field that can support consistent gas flow to the showerhead and consequently to the substrate surface. Uniform distribution can be critical for high-quality and uniform deposition of thin films because it can ensure that all substrate zones are under similar flow and chemical environments. (Fig 4.1(a)) (ii)Baffle:

The baffle acts as a flow-conditioning component, typically placed between the showerhead and the substrate. Its function is to control or diffuse the incoming gas flow, reduce jet impingement, and promote laminar or controlled flow distribution. Proper baffle design helps in suppressing recirculation zones and improving flow uniformity, thereby contributing to more homogeneous film deposition. (Fig. 4.1(a))

(iii)Substrate:
The substrate is the surface onto which the thin film is deposited. It is usually mounted on a heated stage to promote chemical reactions of the gas-phase precursors. The position, temperature, and orientation of the substrate are crucial, as they affect the reaction kinetics, deposition rate, and film quality. Uniform exposure to reactive species is vital for achieving high-performance coatings or semiconductor layers. (Fig. 4.1(a))

(iv)Showerhead:

The showerhead is responsible for delivering precursor gases uniformly across the substrate surface. Its design-particularly the size, number, and distribution of holes-affects the flow rate, velocity profile, and mixing behaviour of gases. A well-optimized showerhead ensures uniform gas distribution, which is essential for achieving consistent film thickness and minimizing defects across the wafer (Fig. 4.1(b)). As shown in Table 4.1, the holes are placed in concentric rings with increasing diameters and distances from the centre. The number of holes per ring increases outward, ranging from 8 to 36.

$$\text{Step size}=\frac{400}{8} = 50mm$$

The area analysis ensures that the number and size of holes are carefully balanced to maintain a uniform flow rate while avoiding localized over-deposition. Table 4.2 quantifies the area of holes in each ring, using the formula:

$$A=N.\frac{\pi D^2}{4}$$

where N is the number of holes and D is the diameter of each hole. The total hole area across all rings is 57,600.87 mm².

To evaluate distribution effectiveness, Table 4.3 compares the total area of holes in each ring with the corresponding annulus area. The total annulus area is 57583.166 mm².The results show that hole area nearly equals the annulus area in all rings, with minimal deviation. This indicates a dense and uniform hole distribution, ensuring consistent gas delivery across the substrate surface.

Table 4.1: Area Analysis of Hole Distribution on a Circular Showerhead with Logarithmic Diameter Pattern (i= 4)

Showerhead (i=4)	Ring	No.of holes	Diameter of holes(mm)	Diameter from centre(mm)
Øln(0+i)*10	1	0	13.8	0

Øln(1+i)*10	2	8	16.09	50
Øln(2+i)*10	3	12	17.9	100
Øln(3+i)*10	4	16	19.4	150
Øln(4+i)*10	5	24	20.7	200
Øln(5+i)*10	6	24	21.9	250
Øln(6+i)*10	7	36	23.0	300
Øln(7+i)*10	8	36	23.9	350

Table 4.2: Area Analysis of Hole Distribution in N ring of the showerhead

Ring	Diameter of hole(mm)	No. of holes	Holes area(mm^2)	Total area(mm^2)
2	16.09	8	203.33	1626.64
3	17.9	12	251.64	3019.79
4	19.4	16	295.59	4729.47
5	20.7	24	336.53	8076.84
6	21.9	24	376.68	9040.43
7	23.0	36	415.475	14957.12
8	23.9	36	448.62	16150.58

Table 4.3: Comparison of area of annulus and total area of holes in N ring of the showerhead

Annulus	Diameter of hole(mm)	No. of holes	Holes area(mm^2)	Ring radius	Rinner (mm)	Router (mm)	Area of the annulus (mm^2)	Total area of holes in N ring(mm^2)
1	16.09	8	203.33	25	19.82	30.175	1625.77	1626.64
2	17.9	12	251.64	50	45.195	54.805	3019.07	3019.79

3	19.4	16	295.59	75	69.98	80.015	4726.526	4729.47
4	20.7	24	336.53	100	93.575	106.425	8073.89	8076.84
5	21.9	24	376.68	125	119.25	130.75	9039.93	9040.43
6	23.0	36	415.475	150	142.07	157.93	14947.69	14957.12
7	23.9	36	448.62	175	167.66	182.35	16150.29	16150.58

4.1.2. Specifications for the HCVD chamber

Table4.4: Geometric details of the HCVD Chamber [2]

Component	Diameter(mm)
Inlet	80
Baffle	16
Substrate	400
Showerhead	400

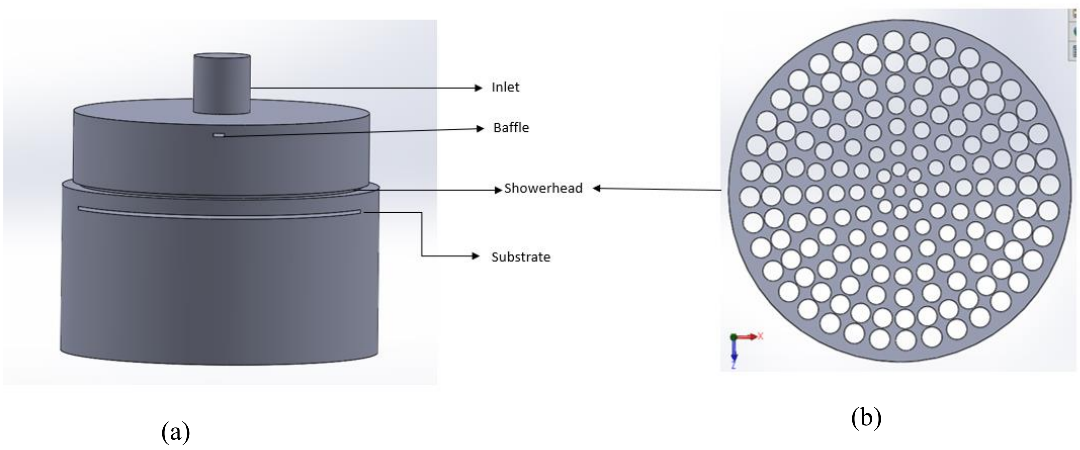

Fig. 4.1:(a) Computational Domain of the 3D Halogen Chemical Vapor Deposition (HCVD) Chamber(b)Showerhead (i=4)

4.1.3. Computational domain of the 2D Halogen Chemical Vapor Deposition (HCVD) Chamber

To optimize computational efficiency without compromising accuracy, a wedge-shaped geometry was employed (Fig. 4.3). This axisymmetric approximation significantly reduces the overall computational cost while effectively capturing the essential flow features in the CVD reactor.

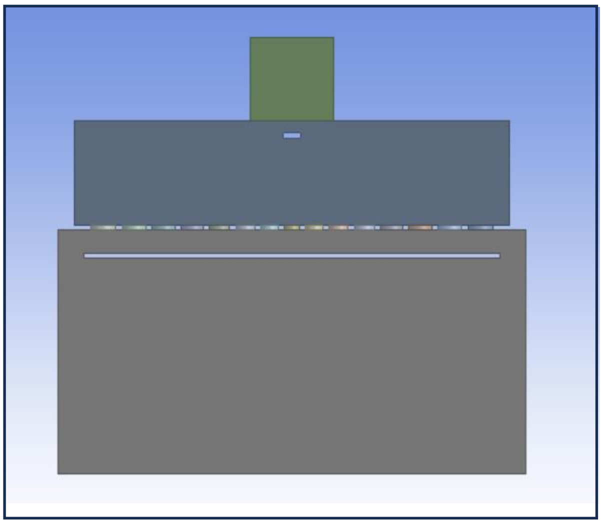

Fig. 4.2: Computational Domain of the 2-D Halogen Chemical Vapor Deposition (HCVD) Chamber

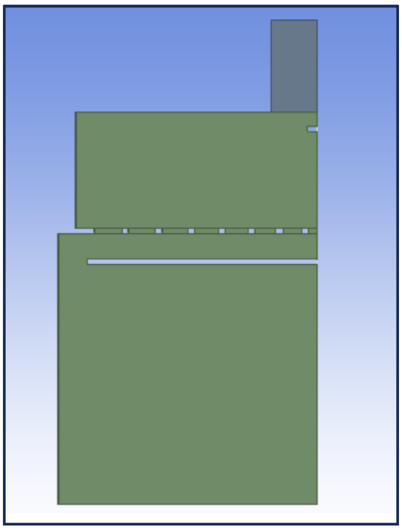

Fig. 4.3: Computational Domain of the axis symmetric 2-D Halogen Chemical Vapor Deposition (HCVD) Chamber (wedge angle is 5^0)

4.2. Meshing of the 2-D Halogen Chemical Vapor Deposition chamber

The computational domain was meshed using SnappyHexMesh, a mesh generation tool in OpenFOAM. The snappyHexMesh utility generates 3D meshes containing hexahedra and split hexahedra from a triangulated surface geometry in Stereolithography (STL) format. The mesh is generated from a dictionary file named snappyHexMeshDict located in the system directory and a triangulated surface geometry file located in the directory constant/ triSurface. The total number of elements generated was 998,611 with a refined mesh density near critical regions such as the showerhead and substrate, where accurate flow resolution is essential.

SnappyHexMesh Workflow

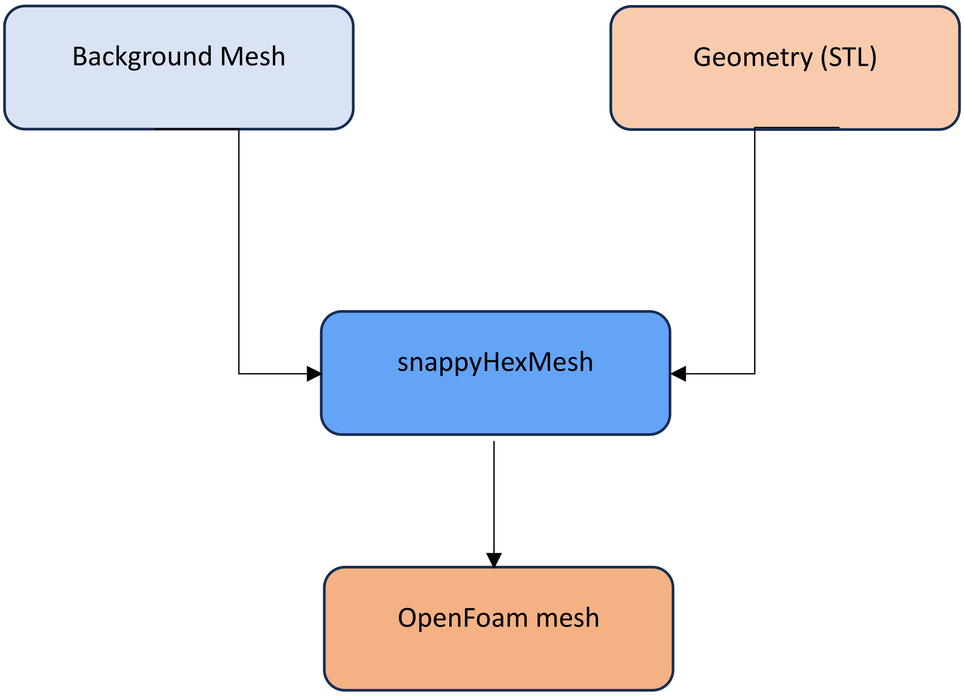

Background mesh
The background mesh is generated using the blockMesh.
The mesh is consists of purely hexes.
The cell aspect ratio should be approximately 1, at least near the STL surface.

snappyHexMesh workflow - Geometry (STL file)
The STL file was generated using the multiple surfaces to accurately represent the geometry of the model for use in the meshing process.
In the case of a STL file with multiple surfaces, we can use local refinement in each individual surface. This gives us more control when generating the mesh.
The STL geometry is always located in the directory constant/triSurface
snappyHexMesh workflow
• The meshing utility snappyHexMesh reads the dictionary snappyHexMeshDict located in the directory system.
• The castellation, snapping, and boundary layer meshing steps are controlled by the dictionary snappyHexMeshDict.
• The final mesh should be always located in the directory constant/polyMesh

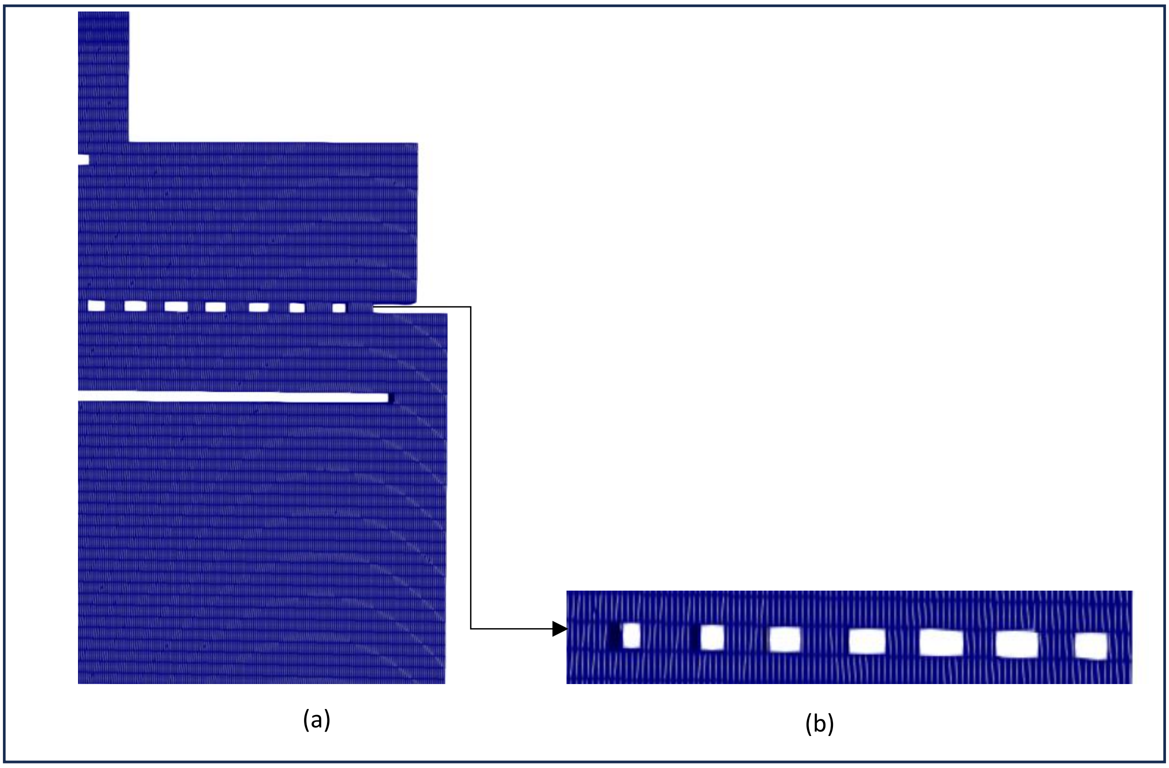

Fig. 4.4: a) Meshing of the axis-symmetric 2-D Halogen Chemical Vapor Deposition (HCVD) Chamber (wedge angle is 5^0)

(b)Zoomed view of the showerhead

4.3. Solver setup

The flow simulation was performed using the existing simpleFoam solver, a steady-state, pressure-based solver for incompressible and laminar flow, available in OpenFOAM v7. It utilizes the SIMPLE (Semi-Implicit Method for Pressure-Linked Equations) algorithm to solve the governing equations efficiently.

For post-processing and visualization of the results, ParaView v5.6.7 was used. It enabled detailed analysis of flow patterns, velocity profiles, and pressure distribution within the reactor domain.

The initial boundary conditions for the cases are listed below in Table 4.5,4.6,4.7.

Table4.5: Pressure Boundary Conditions for the Halogen Chemical Vapor Deposition (HCVD) Chamber [2]

Boundary Field	Type	value
Inlet	ZeroGradient	

Outlet	fixedValue	10000pa
Wedge1	wedge	
wedge2	wedge	
Wall	ZeroGradient	
Sbs(showerhead_Baffle_Substrate)	ZeroGradient	

Table4.6: Velocity Boundary Conditions for the Halogen Chemical Vapor Deposition (HCVD) Chamber [2]

Boundary Field	Type	value
Inlet	fixedValue	0.66 m^2/s
Outlet	ZeroGradient	
wedge1	wedge	
wedge2	wedge	
walls	noSlip	
Sbs(showerhead_Baffle_ Substrate)	noSlip	

Table4.7: molar mass of three different gases

Gas	Molar Mass(kg/mol)
$SiCl_4$	0.169.9
CH_4	0.01604
H_2	0.002016

5. Result and Discussion

To assess the influence of chamber design on flow uniformity over the substrate, two different configurations were simulated and analysed. The objective was to determine how the presence of a showerhead, baffle, and geometric parameters influence gas distribution across the wafer surface in a CVD reactor.

1. Effect of showerhead hole configuration on flow uniformity

In Fig. 5.1(a), the velocity magnitude contour illustrates the flow behaviour inside the CVD chamber when no showerhead and baffle is present. In this baseline configuration, the inlet jet flows directly toward the substrate without any form of redistribution or obstruction. As a result, a strong and focused jet impinges directly at the centre of the substrate, leading to a highly non-uniform velocity distribution. The central region experiences high velocity (up to 0.66 m/s), while the surrounding areas, particularly near the substrate edges, exhibit significantly lower velocities. This uneven flow distribution is undesirable for processes such as thin-film deposition, where uniform exposure across the entire substrate surface is critical. The lack of a showerhead or baffle means that the gas does not spread laterally before reaching the substrate, resulting in concentrated momentum in the central region and minimal flow toward the periphery. Additionally, some recirculating zones can be observed near the upper corners of the chamber; however, they do not contribute meaningfully to improving flow uniformity at the substrate level. This case highlights the inherent limitations of a direct-jet configuration and underscores the need for flow-conditioning elements to achieve uniform coverage across the substrate.

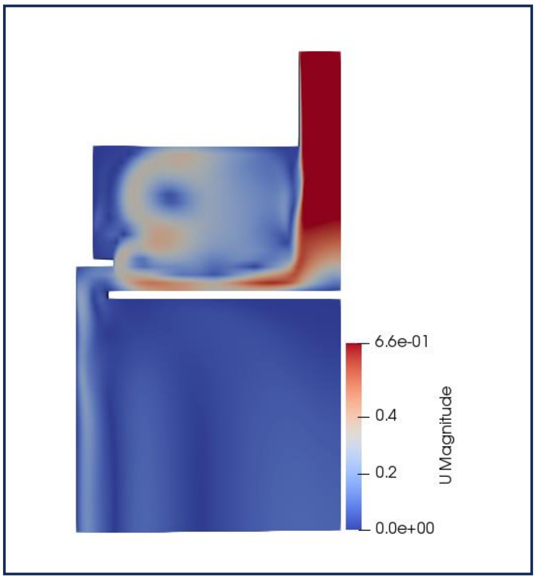

Fig. 5.1: Velocity contour of the axis-symmetric 2-D Halogen Chemical Vapor Deposition (HCVD) Chamber Without showerhead and baffle.

2. Effect of baffle configuration on flow uniformity

In this case, two baffle sizes 8 mm (Fig. 5.2) and 16 mm (Fig. 5.3) were considered to study their effect on the flow distribution. In the case of the Fig. 5.2(a), the smaller obstruction allowed the central high-velocity jet to pass with minimal deflection. As a result, the impinging jet retained a strong axial component, leading to a concentrated flow at the centre of the substrate and poor flow distribution across the surface. The recirculation zones beneath the baffle were weak, and the flow failed to spread effectively in the radial direction. The plot in Fig. 5.2 (b) shows the Y-component of velocity (Uy) as a function of radial position on the substrate. The Uy profile is highly non-uniform, featuring multiple local maxima and minima across the 0-0.2 m radius range. The central region ($r < 0.04$ m) shows positive Uy values, peaking near +0.22 m/s, indicating strong downward momentum. However, this is quickly followed by negative Uy values (up to -0.65 m/s), particularly in the outer region ($r \approx 0.16$-0.2 m), implying reverse flow or upward recirculation at the substrate edge. Such oscillatory behaviour in Uy reflects a lack of smooth radial velocity decay, suggesting complex vortical structures and poor gas flow uniformity at the deposition surface. These fluctuations can severely degrade film quality by inducing thickness non-uniformity, inconsistent precursor flux, and localized turbulence.

On the other hand, the Fig. 5.3(a) provided a larger surface area to obstruct and redirect the incoming jet. This led to a more diffused flow pattern as the jet was forced to spread laterally before reaching the showerhead and subsequently the substrate. As a result, the velocity gradients across the substrate were comparatively smoother, and the flow showed better radial uniformity. Although the central impingement was still present, it was less dominant than in the 8 mm case. This suggests that increasing the baffle size enhances the redistribution of momentum and improves the overall flow uniformity on the substrate surface. The plot in Fig. 5.3 (b) presents the plot of the Y-component of velocity (Uy) against the radial position on the substrate. The entire profile lies in the negative Uy region, indicating a net downward flow throughout the substrate area, which is physically expected in a CVD process. However, the velocity distribution is highly non-uniform, with notable fluctuations and multiple local minima and maxima across the radius. From approximately 0.12 m to 0.20 m, the profile exhibits steep negative gradients, with Uy dropping below -0.25 m/s, suggesting localized regions of high axial momentum toward the edge. These spikes could be the result of vortex-induced flow concentration or secondary jet interactions emerging from incomplete gas diffusion. In the central region (0-0.08 m), the Uy remains relatively shallow, indicating slower vertical flow and possibly inadequate precursor transport to that area.

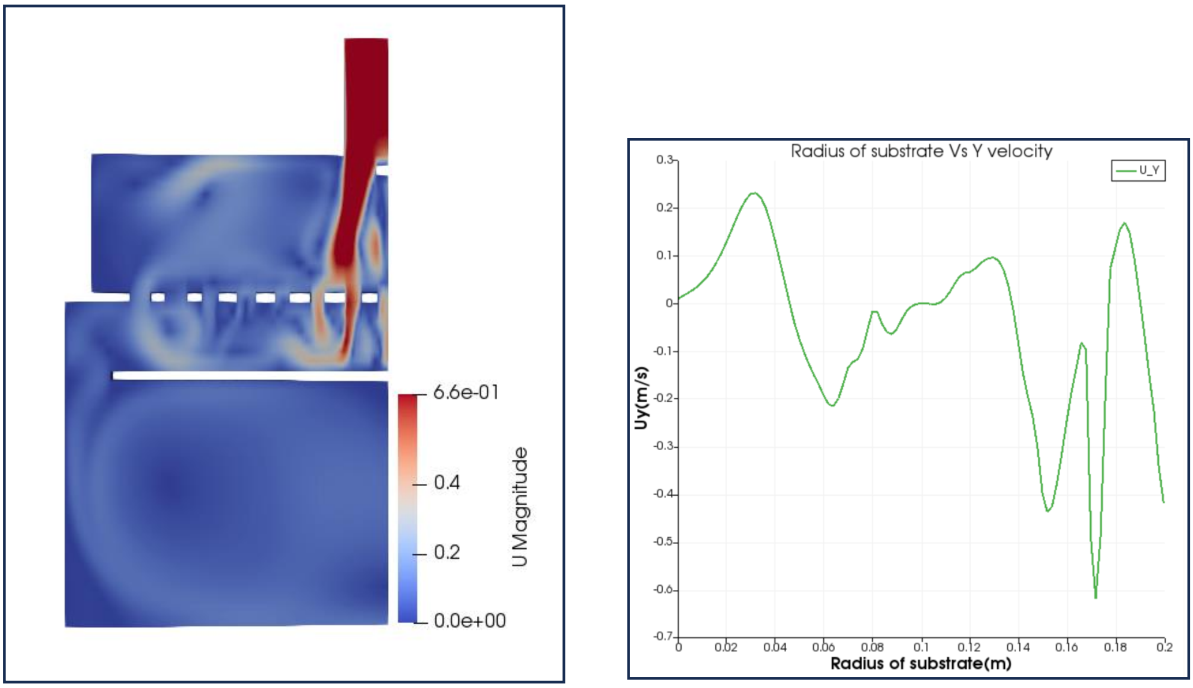

(a) (b)

Fig. 5.2: Velocity contour of the axis-symmetric 2-D Halogen Chemical Vapor Deposition (HCVD) Chamber for baffle diameter (a) D=8mm (b) plot of Y-component of velocity (Uy) across the substrate radius

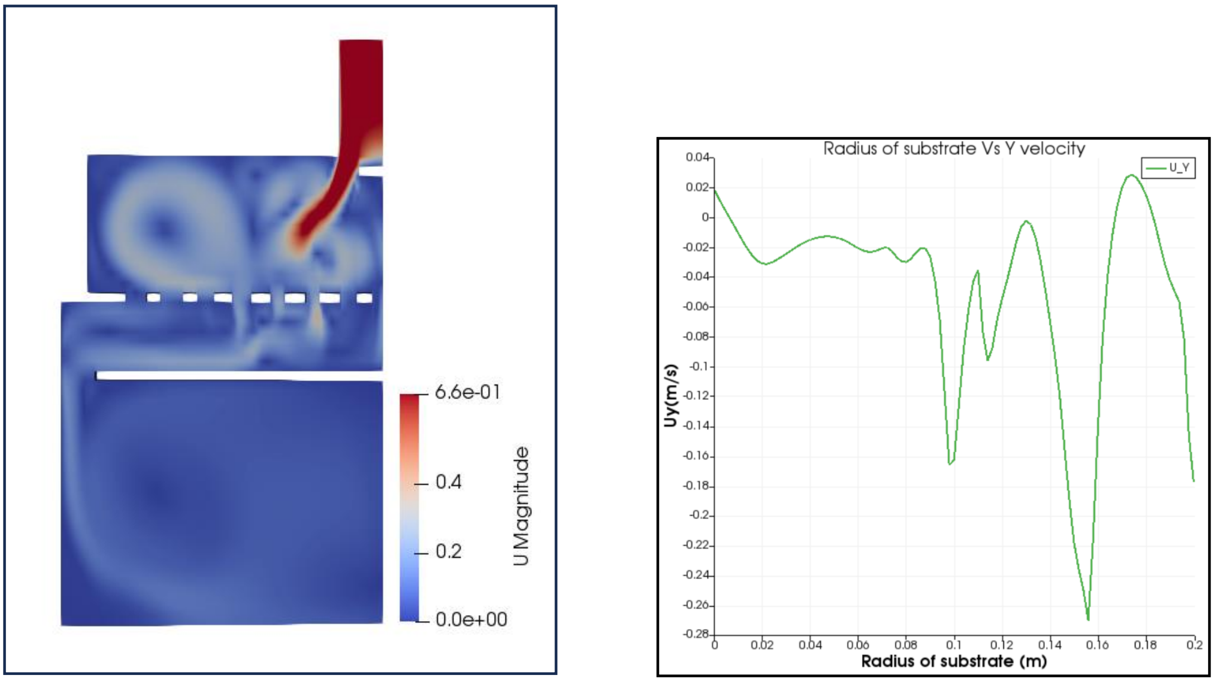

(a) (b)

Fig. 5.3: Velocity contour of the axis-symmetric 2-D Halogen Chemical Vapor Deposition (HCVD) Chamber for baffle diameter (a) D=16mm (b) plot of Y-component of velocity (Uy) across the substrate radius

3. Effect of substrate configuration on flow uniformity

Fig. 5.4(a) presents the velocity magnitude contour for the axisymmetric 2D HCVD chamber with the substrate placed at 50 mm from the showerhead, compared to the earlier configurations where it was located at 100 mm. With the reduced chamber height, the substrate is positioned closer to the gas injection zone, which significantly affects the flow development. The velocity contour reveals that the high-momentum jet emanating from the inlet and showerhead interacts more directly with the substrate surface due to reduced vertical distance. The velocity profile near the baffle shows incomplete radial dispersion, with a stronger axial component retained in the core region. This configuration limits the residence time available for the gas to diffuse and redistribute, resulting in localized regions of high velocity impingement near the central axis and increased shear gradients. Furthermore, the proximity of the substrate restricts the space available for flow to stabilize and suppresses the formation of fully developed laminar profiles. The lower chamber shows relatively weak flow and minimal recirculation, with possible dead zones that could hinder deposition efficiency.

Fig. 5.4(b) illustrates the Y-component of velocity (Uy) as a function of the radial position on the substrate for the configuration with the substrate positioned at 50 mm below the showerhead. The velocity profile exhibits pronounced non-uniformity, with both positive and negative Uy values distributed across the substrate radius, indicating significant axial flow variation. Near the central region ($r < 0.02$ m), Uy values are slightly positive, suggesting weak downward flow and insufficient precursor momentum. As the radial distance increases ($r =$ 0.04-0.16 m), Uy fluctuates between small negative values in the range of approximately -0.05 to -0.25 m/s, representing mild axial transport accompanied by flow instabilities. Toward the outer edge of the substrate ($r \approx$ 0.18-0.20 m), Uy undergoes a sharp decline, reaching values below -0.4 m/s, which signifies strong localized downward flow likely resulting from redirected central jets or peripheral recirculation effects. These steep gradients and abrupt transitions in Uy indicate a non-uniform gas delivery pattern, where higher axial velocities are concentrated near the substrate edges, while the central zones experience weaker and less directed flow. Such behaviour is attributed to the limited vertical spacing between the showerhead and substrate, which restricts the development of a fully diffused and radially balanced flow field. As a result, the precursor gases do not undergo sufficient spatial redistribution before reaching the deposition surface, leading to uneven species transport. This flow non-uniformity is detrimental to achieving consistent film thickness and can introduce defects or composition gradients in the deposited layer, underscoring the critical influence of substrate placement on deposition uniformity in HCVD systems.

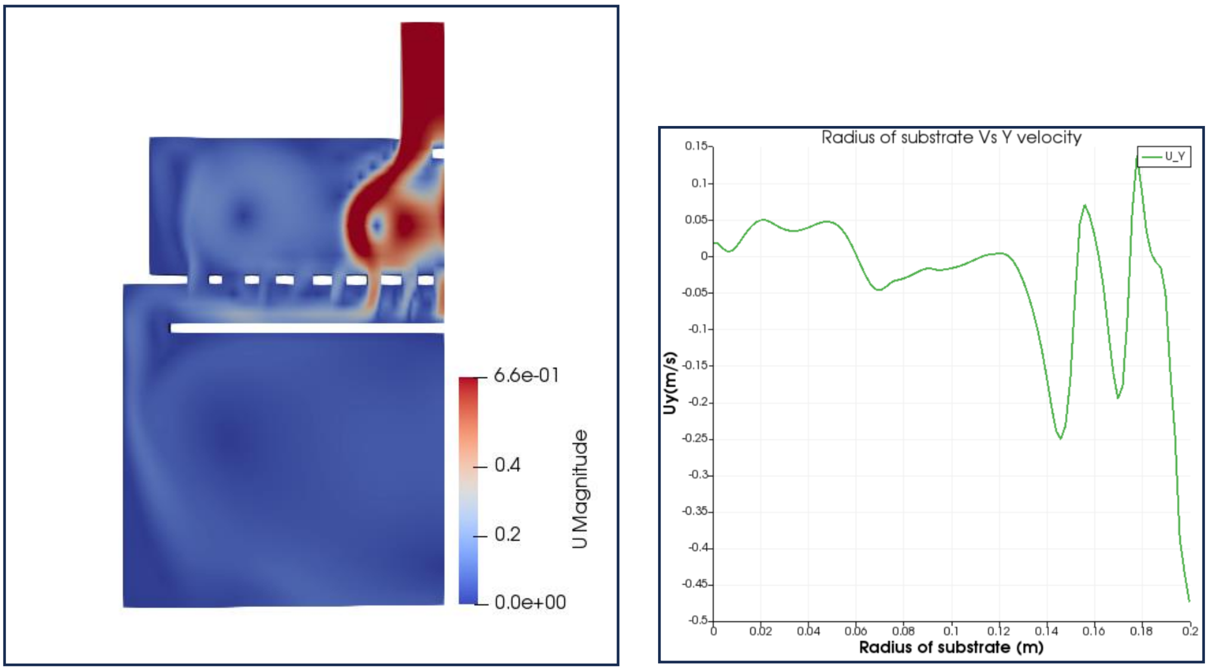

(a) (b)

Fig. 5.4: Velocity contour of the axis-symmetric 2-D Halogen Chemical Vapor Deposition (HCVD) Chamber for (a) substrate positioned at 50 mm, and (b) plot of Y-component of velocity (Uy) across the substrate radius.

6. Conclusion

This study systematically evaluated the effects of showerhead design, baffle diameter, and substrate positioning on gas flow uniformity within an HCVD chamber. Initial results showed that the absence of a showerhead or baffle leads to severe jet impingement and highly non-uniform velocity distribution at the substrate surface. The incorporation of a showerhead improved gas redistribution but failed to eliminate the dominance of axial flow along the centerline. Among the baffle configurations tested, the 16 mm diameter baffle demonstrated superior performance over the 8 mm variant by effectively diffusing incoming flow and promoting lateral gas spreading. These findings highlight the significant influence of both geometric and operational parameters on flow behaviour within the CVD reactor. The CFD simulations performed using OpenFOAM provide a rigorous and scalable framework for optimizing reactor configurations, enabling improved flow uniformity, reduced defect formation, and enhanced process yield in semiconductor manufacturing.

7. Acknowledgement

I would like to extend my deepest gratitude to my supervisors, Dr. Ajit, Prof. Himani Garg and Prof. Raghuvendra Gupta, for their unwavering support and insightful feedback throughout the course of this study. Their combined corporate and academic expertise, along with their meticulous attention to detail, made this learning experience both enriching and exemplary. I am sincerely thankful to my FOSSEE mentor, Mr. Manjil Sitoula, whose consistent guidance helped me navigate challenges and stay focused on the successful completion of this project.

References

1. Lee, G., Sohn, D. K., Seok, S. H., & Ko, H. S. (2019). The effect of hole density variation in the PECVD reactor showerhead on the deposition of amorphous carbon layer. *Vacuum*, *163*, 37-44.
2. Li, Q., Zhang, Y., Ji, B., Zhang, S., & Tu, R. (2023). Improvement of SiC deposition uniformity in CVD reactor by showerhead with baffle. *Journal of Crystal Growth*, *615*, 127255.
3. Jin, Z., Lim, D. D., Zhao, X., Mamunuru, M., Roham, S., & Gu, G. X. (2024). Machine learning enabled optimization of showerhead design for semiconductor deposition process. *Journal of Intelligent Manufacturing*, *35*(2), 925-935.
4. Choo, J. O., Adomaitis, R. A., Rubloff, G. W., Henn-Lecordier, L., & Liu, Y. (2005). Simulation-based design and experimental evaluation of a spatially controllable CVD reactor. *AIChE journal*, *51*(2), 572-584.
5. Kim, H. J., & Yoon, J. H. (2021). Computational fluid dynamics analysis of particle deposition induced by a showerhead electrode in a capacitively coupled plasma reactor. *Coatings*, *11*(8), 1004
6. Zhang, T., Zhang, J., Shen, B., & Sun, F. (2012). Simulation of temperature and gas density field distribution in diamond films growth on silicon wafer by hot filament CVD. *Journal of crystal growth*, *343*(1), 55-61.
7. Geiser, J., & Arab, M. (2011). Modeling and simulation of a chemical vapor deposition. *Journal of Applied Mathematics*, *2011*(1), 641920.
8. Xia, H., Xiang, D., & Mou, P. (2014). Simulation-based optimization of a vector showerhead system for the control of flow field profile in a vertical reactor chamber. *Advances in Mechanical Engineering*, *6*, 525102.
9. Zheng, G., Sun, Y., Liu, S., Su, P., Pei, J., Zuo, R., & Liu, L. (2025). Numerical investigation on the effect of growth conditions on silicon carbide growth in chemical vapor deposition. *Journal of Crystal Growth*, *657*, 128108.